Biochimica et Biophysica Acta, 986 (1988) 75–82
Elsevier

BBAMEM 74628

The effects of dansylation on the pH dependence of SO_4^{2-} and Cl^- equilibrium exchange and on the H^+/SO_4^{2-} cotransport across the red blood cell membrane

A. Berghout *, M. Raida, B. Legrum and H. Passow

Max-Planck-Institut für Biophysik, Frankfurt am Main (F.R.G.)

(Received 23 March 1989)
(Revised manuscript received 21 July 1989)

Key words: Anion transport; Erythrocyte membrane; Dansyl chloride; Band 3 protein; Cotransport

Treatment of the erythrocyte membrane with dansyl chloride leads to the following effects: (i) SO_4^{2-} transport is enhanced, Cl^- transport is reduced. At maximal acceleration of sulfate exchange, Cl^- exchange is only partially inhibited. The two effects are linearly related suggesting that the Cl^- and SO_4^{2-} transporting forms of band 3 are derived from the same pool. (ii) The maximum of the pH dependence of SO_4^{2-} equilibrium exchange as measured at low sulfate concentrations is replaced by a plateau. It now resembles the pH dependence of Cl^- exchange in untreated red cells. The pH dependence of SO_4^{2-} equilibrium exchange as measured at high sulfate concentrations is virtually unchanged after dansylation. The pH dependence of the partially inhibited Cl^- equilibrium exchange across the dansylated membrane as measured at high chloride concentrations remains similar as in the untreated red cells but is somewhat less pronounced. (iii) SO_4^{2-}/H^+ cotransport remains essentially unaltered after modification by dansyl chloride. The effects of dansylation are discussed in terms of a model similar to the titratable carrier model originally proposed by Gunn (Gunn, R.B. (1972) in Oxygen Affinity of Hemoglobin and Red Cell Acid Base Status (Rorth, M. and Astrup, P., eds.), pp. 823–827, Munksgaard, Copenhagen).

Introduction

Much attention has been paid to the relationship between the transport across the erythrocyte membrane of monovalent anions such as Cl^- and divalent anions such as SO_4^{2-}. Most reagents studied sofar inhibit Cl^- and SO_4^{2-} transport to the same extent if measured under identical conditions [1]. One exception, however, is the covalent chemical modification of the red cell membrane with dansyl chloride which produces reciprocal effects on monovalent and divalent anion transport: Cl^- transport measured at 0°C is decreased and SO_4^{2-} transport measured at 30°C is enhanced [2]. Both effects are augmented when dansylation is carried out in the presence of the disulfonic acid APMB, an inhibitor of anion transport which binds reversibly to the same site at which H_2DIDS combines with the protein.

Dansyl chloride penetrates easily across the red blood cell membrane and is capable of reacting with amino acid residues carrying amino, imidazole, -SH and phenolic -OH groups [3]. In addition to hemoglobin, all membrane proteins that can be separated by one-dimensional SDS-polyacrylamide gel electrophoresis, as well as the aminolipids, become fluorescently labeled [4]. In contrast to DANS-Cl, the water-soluble derivative PENS-Cl does not penetrate through the membrane and labels the red cell membrane proteins only very little. However, the labeling of band 3 protein in resealed ghosts is too weak to localize the modified amino acid residues by fluorescence measurement [5].

Although the transport across the red blood cell membrane of both monovalent and divalent inorganic anions seems to be mediated by the band 3 protein, the kinetics of the transport of the two types of anion species differ in many respects [6–9]. Most conspicuous is the difference in pH dependence: The rate of Cl^- transport as measured at temperatures below 15°C,

* Present address: Institut für Pharmakologie und Toxikologie, Philipps Universität, K.-v.-Frischstrasse, Marburg, F.R.G.

Abbreviations: APMB, 2-(4-aminophenyl-3-sulfonic acid)-6-methylbenzothiazol-7-sulfonic acid; DANS-Cl, dansyl chloride(5-dimethylaminonaphthyl-1-sulfonyl chloride); H_2DIDS, 4,4′-diisothiocyanatodihydrostilbene-2,2′-disulfonic acid; PENS-Cl, 2-(*N*-piperidine)ethylamine-1-naphthyl-5-sulfonyl chloride; TCA, trichloroacetic acid.

Correspondence: H. Passow, Max-Planck-Institut für Biophysik, Heinrich-Hoffmann-Strasse 7, 6000 Frankfurt/M.71, F.R.G.

increases with increasing pH until, above pH 7.0, a plateau is reached which extends up to at least pH 11.0 [10]. At more elevated temperatures, Cl^- transport passes through a relatively flat maximum above pH 7.0 [11]. Between 4 and 37 °C, SO_4^{2-} transport passes through a pronounced maximum around pH 6.0–6.5 [12,13].

The titratable carrier model (Fig. 1) proposed by Gunn offered an explanation for the difference between the pH dependence of monovalent and divalent anion transport [14–16]. The model states that the inhibition of Cl^- transport and the enhancement of SO_4^{2-} transport at increasing H^+ concentration, depend on the protonation of one single H^+ binding site. Protonation of this site converts the anion transporter from a carrier for monovalent anions into a carrier for divalent anions. The protonated form of the transporter accomplishes a cotransport of one H^+ together with one divalent anion [17].

Although the binding of dansyl chloride to the erythrocyte membrane is quite non-specific, the effect of dansylation on anion transport shows highly specific features [2,18,19]. In the present study, we made use of the striking difference of the effects of dansylation on the equilibrium exchange of Cl^- and SO_4^{2-} to investigate the relationship between the pH dependence of monovalent and divalent anion transport. The experiments presented below deal with the effect of dansylation on the relationship between H^+/SO_4^{2-} cotransport and SO_4^{2-} equilibrium exchange and with the relationship between the pH dependence of SO_4^{2-} and Cl^- equilibrium exchange. The results are discussed in terms of an extended form of the titratable carrier model originally proposed by Gunn [14].

Materials and Methods

Anion equilibrium exchange was measured in red blood cell ghosts prepared as described by Schwoch and Passow [20]. The hemolysis ratio was 1:50 and the hemolysis medium contained 4 mmol/l $MgSO_4$, 0.5 mmol/l acetic acid; the temperature at hemolysis was 0 °C. Resealing, dansylation, and subsequent flux measurements were carried out in a 'standard medium' containing 1 mmol/l Na_2SO_4, 130 mmol/l NaCl, 20 mmol/l EDTA, unless stated otherwise. During resealing the pH was 7.4. Modification with DANS-Cl and PENS-Cl in the standard medium in the presence of 5 mmol/l of the potentiating agent APMB, was performed as described by Legrum et al. [18] and Raida and Passow [5], respectively. Prior to the measurement of Cl^- equilibrium exchange, the pH was equilibrated by two or three washes in standard media of the appropriate pH before the ghosts were loaded with $^{36}Cl^-$. The efflux of Cl^- in standard medium at 0 °C was measured by means of the inhibitor-stop method as described by Ku et al. [1]. In the experiments at 4 °C, the filtration technique as described by Dalmark and Wieth [21] was used. SO_4^{2-} equilibrium exchange was measured in standard medium after loading the ghosts with $^{35}SO_4^{2-}$ at pH 6.6 (45 min, 37 °C). The ghosts were then washed free of extracellular $^{35}SO_4^{2-}$ in icecold media of the appropriate pH and resuspended in these media at a hematocrit of 1% and a temperature of 30 °C. Control experiments have shown that the presence of HCO_3^- from the air ensures the pH equilibration between ghosts and medium during the washes provided the hematocrit is less than about 2%. The appearance of $^{35}SO_4^{2-}$ in the supernatant was followed

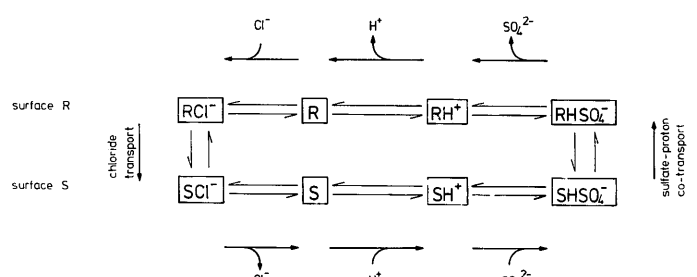

Fig. 1. Titratable carrier model of anion transport. R and S represent the conformation of the transporter with its empty transfer site facing surface R and S, respectively. The thick arrows represent the cycle of Cl^-/SO_4^{2-} net exchange. The thin arrows in the middle of the figure represent the pathway of equilibrium exchange. For further explanation see text.

and rate constants were calculated as described by Legrum et al. [18]. The ghost volume distribution was measured by means of a Coulter Counter with a hydrodynamic focussing system [22]. The ghost volume is independent of pH over the pH range 8.5–6.8. There is a tendency of an increase in volume at pH values below this range which amounts to maximally 15–20% at pH 5.5. The rate constants given in the figures and the text were corrected for this effect.

Measurement of SO_4^{2-}/H^+ cotransport

For the measurement of SO_4^{2-}/H^+ cotransport, ghosts were prepared containing 130 mmol/l NaCl, 1 mmol/l Na_2SO_4, 40 mmol/l EDTA. Dansylation was performed in this medium with 0.125 mmol/l DANS-Cl in the presence of 5 mmol/l APMB. After the removal of APMB and breakdown products, the ghosts were equilibrated in isoosmotic media containing either 170 mmol/l NaCl, 45 mmol/l sucrose or 140 mmol/l Na_2SO_4, 45 mmol/l sucrose. Other ghosts containing 130 mmol/l NaCl, 1 mmol/l Na_2SO_4, 20 mmol/l EDTA were modified in this medium with 0.25 mmol/l PENS-Cl in the presence of 5 mmol/l APMB. After removal of APMB and breakdown products, these ghosts were equilibrated with isoosmotic media containing either 160 mmol/l NaCl or 140 mmol/l Na_2SO_4. Unmodified ghosts were prepared similarly, except that no DANS-Cl or PENS-Cl was added to the media during the modification period. The H^+ efflux was measured in an airtight chamber by injecting 0.10 ml of packed ghosts that were equilibrated with media containing SO_4^{2-} as the only penetrating anion species into 15 ml of an unbuffered, isoosmotic medium containing Cl^- as the only permeating anion species. The media were made HCO_3^--free by flushing vigorously with 99.996% N_2 for at least 30 min [17]. The cells were made HCO_3^--free in a dialysis bag by equilibration with N_2-flushed medium for at least 30 min. Shortly before the H^+ flux measurement, the pH of the medium was adjusted to the pH of the cell suspension with N_2-flushed, diluted H_2SO_4 or NaOH. Vice versa, H^+ influx measurements were performed by injecting ghosts containing only Cl^-, in media containing only SO_4^{2-} as the permeable anion species.

Results

Relationship between the effect of dansylation on Cl^- and SO_4^{2-} equilibrium exchange

All experiments were performed with resealed human red blood cell ghosts. Prior to the flux measurements, the ghosts were treated with dansyl chloride (DANS-Cl) under standard conditions (DANS-Cl at the desired concentration in 130 mmol/l NaCl, 1 mmol/l Na_2SO_4, 20 mmol/l EDTA, pH 6.6) in the presence of a potentiating agent, APMB [2]. After modification, the unreacted DANS-Cl, its hydrolysis products, and the APMB were removed by washing. Subsequently, the ghosts were equilibrated in the required media, usually of the composition indicated above, except that the pH was 7.4. In accord with previous observations, H_2DIDS reduces the rate of anion exchange to the same low level in the dansylated as in the untreated cells. The data presented below only refer to rates corrected for the H_2DIDS-insensitive flux component.

The effect of dansylation at various DANS-Cl concentrations on Cl^- and SO_4^{2-} transport tends to approach a plateau after treatment at DANS-Cl concentrations of 0.125 mmol/l or more (Fig. 2). The H_2DIDS-sensitive SO_4^{2-} flux is enhanced about 25-fold while the H_2DIDS-sensitive Cl^- flux is reduced to 47% of its control value. When the effects on Cl^- and SO_4^{2-} transport are plotted against each other, the data points scatter around a straight line (Fig. 3). This would be in keeping with the view that dansylation augments the transport of SO_4^{2-} at the expense of Cl^- transport.

pH dependence of SO_4^{2-} equilibrium exchange after dansylation

Measured at low sulfate concentrations, the pH dependence of SO_4^{2-} equilibrium exchange across the dansylated membrane as compared to untreated controls changes (Fig. 4): The maximum at pH 6.5 disappears and is replaced by a plateau that extends from pH 8.0 up to at least pH 8.5. After dansylation, the pH dependence of SO_4^{2-} equilibrium exchange now resembles the pH dependence of Cl^- equilibrium exchange. In terms of the titratable carrier model this could be the results of an uncoupling of SO_4^{2-}/H^+ cotransport or a change in the apparent pK of the proton binding over several pH units to a more alkaline value after dansylation.

The pH dependence of SO_4^{2-} equilibrium exchange measured at high sulfate concentrations is essentially similar in the dansylated and untreated cells (Fig. 5). However, there is a slight tendency for the dansylated cells to show a somewhat increased rate of exchange, notably at the pH values above the maximum. Due to the limited pH range that is accessible for experimental studies, it was not possible to determine whether the SO_4^{2-} transport at high pH values is fully or only partially inhibited.

pH dependence of Cl^- equilibrium exchange after dansylation

The pH dependence of Cl^- equilibrium exchange across the dansylated membrane as measured at high chloride concentrations is shown in Fig. 6. The inhibited exchange still shows an essentially similar pH dependence as the exchange in the untreated controls. However, the increase of exchange rate up to the plateau level is somewhat reduced and possibly an apparent pK

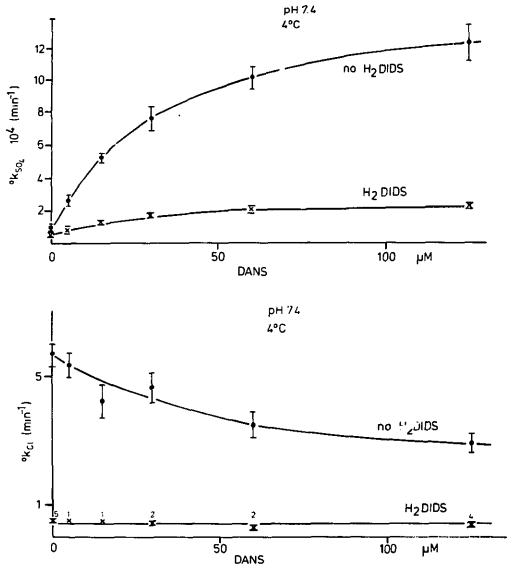

Fig. 2. SO_4^{2-} (top) and Cl^- (bottom) equilibrium exchange at pH 7.4, 4° C in dansylated and unmodified ghosts. Dansyl chloride was added as the cyclodextrin complex in a medium containing 130 mmol/l NaCl, 1 mmol/l Na_2SO_4, 20 mmol/l EDTA, 5 mmol/l APMB and different concentrations of dansyl chloride as indicated on the abcissa. After removal of APMB and breakdown products, $^{35}SO_4^{2-}$ and $^{36}Cl^-$ efflux was measured in the absence or presence (+H_2DIDS) of 0.025 mmol/l H_2DIDS in a medium containing 130 mmol/l NaCl, 1 mmol/l Na_2SO_4, 20 mmol/l EDTA. The error bars represent the S.E. of six experiments unless indicated otherwise by the numbers next to the data points.

value governing the pH dependence is shifted slightly to somewhat more acid pH values. Perhaps after dansylation under more rigorous conditions the pH dependence might completely disappear, we did not try, however, to work out conditions which yield a bigger effect.

SO_4^{2-}/H^+ cotransport after dansylation

Net exchange of SO_4^{2-} with Cl^- in a HCO_3^--free medium results in a SO_4^{2-}/H^+ cotransport [17]. One H^+ and one SO_4^{2-} exchange against one Cl^-. The SO_4^{2-}/H^+ cotransport is measured by injecting red cells containing either Cl^- or SO_4^{2-} as the only penetrating intracellular anion species into unbuffered media containing, respectively, SO_4^{2-} or Cl^- as the only penetrating anion species. In the absence of CO_2, extracellular SO_4^{2-} enters the red cells together with a proton (as HSO_4^-) in exchange for Cl^-. This leads to an increase of the pH in the medium. Intracellular SO_4^{2-} also leaves the red cells together with a proton, which gives rise to a decrease of the pH in the medium. The H^+ movements associated with SO_4^{2-}/Cl^- net exchange can be subdivided into two components. One component is the H^+ flux that accompanies the SO_4^{2-} flux. The other component is an opposing H^+ flux that equilibrates the protons that had been transported together with SO_4^{2-} and possibly consists of a Cl^-/H^+ cotransport. This latter component is much slower than the former and is most apparent after Cl^- and HSO_4^- reached equilibrium [17].

The rather complex time course of the H^+ movements across the erythrocyte membrane could not be determined with high accuracy with the technical possibilities at hand. Using a glass electrode in a well stirred N_2-gassed chamber we obtained some semiquantitative results. They suggest that the fluxes remain essentially

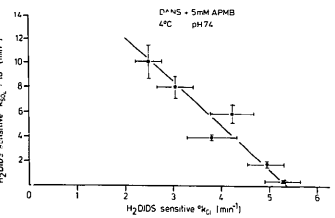

Fig. 3. Relationship between the decrease of Cl^- equilibrium exchange and increase of SO_4^{2-} equilibrium exchange after dansylation in the presence of APMB. Data from the experiments shown in Fig. 2. Abcissa: H_2DIDS sensitive rate constant of Cl^- efflux. Ordinate: H_2DIDS sensitive rate constant of SO_4^{2-} efflux. The error bars represent the S.E. of six experiments. Linear regression analysis of the data points yields the straight line: $^{\circ}k_S = 1.81 \cdot 10^{-3} - 3.29 \cdot 10^{-4} \, ^{\circ}k_{Cl}$ ($r = 0.96$), where $^{\circ}k_S$, $^{\circ}k_{Cl}$ and r represent, respectively, the H_2DIDS-sensitive rate constant of SO_4^{2-} and Cl^- efflux and the correlation coefficient.

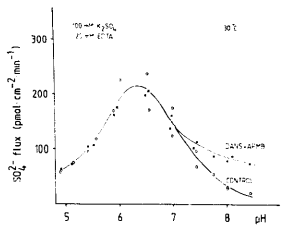

Fig. 5. pH dependence of SO_4^{2-} equilibrium exchange in untreated ghosts (control) and in ghosts that were dansylated with 0.125 mmol/l DANS-Cl in the presence of 5 mmol/l APMB in a medium containing 1 mmol/l K_2SO_4, 20 mmol/l EDTA (DANS+APMB). After removal of APMB and breakdown products, the cells were equilibrated with a medium containing 100 mmol/l K_2SO_4, 20 mmol/l EDTA. SO_4^{2-} efflux was measured in this medium at 30°C and at the pH indicated on the abcissa.

unaltered after dansylation (Fig. 7). These results are in accordance to the observation that the pH dependence of SO_4^{2-} equilibrium exchange measured at high SO_4^{2-} concentrations is virtually unchanged after dansylation and suggest that the H^+/SO_4^{2-} cotransport as measured at high SO_4^{2-} concentrations is not affected by dansylation.

In this context, it may be recalled that dansylation renders the red cell membrane leaky for K^+ and Na^+ [18]. One would expect, therefore, that H^+ may cross the membrane through the newly created cation channels. Such transport of H^+ by a pathway outside band 3 cannot account for the findings described. The proton movements are due to the cotransport since modification of the membrane with the nonpenetrating dansyl derivative PENS-Cl causes the same effects as dansyla-

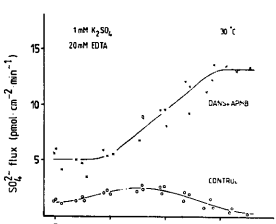

Fig. 4. pH dependence of SO_4^{2-} equilibrium exchange in untreated ghosts (control) and in ghosts that were dansylated with 0.125 mmol/l DANS-Cl in the presence of 5 mmol/l APMB in a medium containing 1 mmol/l K_2SO_4, 20 mmol/l EDTA (DANS+APMB). After removal of APMB and breakdown products, SO_4^{2-} efflux was measured in the same medium at 30°C and at the pH indicated on the abcissa.

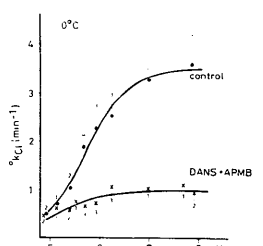

Fig. 6. pH dependence of Cl^- equilibrium exchange in untreated ghosts (control) and in ghosts that were dansylated with 0.125 mmol/l DANS-Cl in the presence of 5 mmol/l APMB in a medium containing 130 mmol/l NaCl, 1 mmol/l Na_2SO_4, 20 mmol/l EDTA (DANS+APMB). After removal of APMB and breakdown products, Cl^- efflux was measured in the same medium at 0°C and the pH indicated on the abcissa. Ordinate: rate constant of Cl^- efflux in minutes. The solid line is calculated by fitting the data points by means of a nonlinear least-squares fitting computer program to the equation $^{\circ}k_{Cl} = V_{max} \cdot K_H / (K_H + H^+)$. The calculated p$K$ for unmodified and dansylated cells amounts 5.71 ± 0.04 and 5.07 ± 0.13, respectively. The calculated V_{max} for unmodified and dansylated cells amounts 3.51 ± 0.10 and 0.99 ± 0.06, respectively.

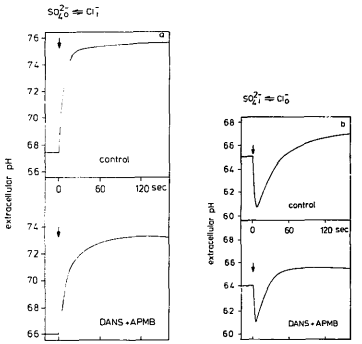

Fig. 7. pH changes associated with the net exchange of extracellular SO_4^{2-} against intracellular Cl^- in untreated ghosts (control) and ghosts that were dansylated with 0.125 mmol/l DANS-Cl in the presence of 5 mmol/l APMB in a medium containing 130 mmol/l NaCl, 1 mmol/l Na_2SO_4, 40 mmol/l EDTA (DANS + APMB). After removal of APMB and breakdown products, the ghosts were equilibrated with an isoosmotic medium that contains only Cl^- or SO_4^{2-} as the main anion species. The measurements were made in the absence of CO_2 by flushing the media with N_2 for at least 30 min. Before the flux measurement, the pH of the cells was adjusted to that of the medium. (a) At the time marked by the arrow, the Cl^--containing cells were injected into a medium that contained only SO_4^{2-} as the main penetrating anion species and the H^+ movements were followed. The increase of pH indicates H^+ uptake by the red cells. (b) At the time marked by the arrow, the SO_4^{2-}-containing cells were injected into a medium that contained Cl^- as the only penetrating anion species and the ensuing pH changes were recorded. The decrease of pH indicates H^+ efflux from the red cells. It is followed by compensatory H^+ movements which are faster than the equilibration of pH in the experiments shown in (a).

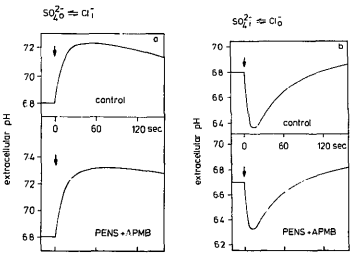

Fig. 8. pH changes associated with the net exchange of extracellular SO_4^{2-} against intracellular Cl^- in untreated ghosts (control) and ghosts that were treated with 0.25 mmol/l PENS-Cl in the presence of 5 mmol/l APMB in a medium containing 130 mmol/l NaCl, 1 mmol/l Na_2SO_4, 20 mmol/l EDTA (DANS + APMB). The other conditions were identical to those described in the legend to Fig. 7.

tion (Fig. 8), even though this compound does not render the membrane permeable to Na^+ or K^+ [5].

Discussion and Conclusions

In the past, Gunn's titratable carrier model formed a most useful conceptual basis for many studies on SO_4^{2-} and Cl^- transport. It became clear, however, that the model needed revision. The earliest and most striking observation that contradicted the model originates from Schnell's laboratory [13]. As pointed out by Knauf [6] and Legrum et al. [18] the titratable carrier model would predict that changes of transport rate should be essentially due to changes of the dissociation constant $K_{1/2}$ for SO_4^{2-} binding as function of pH whilst the maximal transport rate J_{max} should remain unaffected. The data of Schnell et al. [13], however, showed that both $K_{1/2}$ and J_{max} are functions of pH. Later, work from Gunn's laboratory yielded further evidence to this effect [23,24].

The results of the present experiments may be qualitatively described in terms of a model similar to the titratable carrier model originally proposed by Gunn [14]. The model exists of one transfer site for SO_4^{2-} or Cl^-, and two H^+ binding sites. One H^+ binding site inhibits both Cl^- and SO_4^{2-} transport. The second H^+ binding site inhibits Cl^- transport and enhances SO_4^{2-} transport (Fig. 9).

The pH dependence of SO_4^{2-} equilibrium exchange as measured at high SO_4^{2-} concentrations and in the absence of Cl^- retains its characteristic bell-shaped form (Fig. 5). The transport rate at low pH values is the same in dansylated and untreated cells. In terms of the kinetic scheme (Fig. 9), this limiting case is described by

$$J_{max}^{S} = k_{15} \cdot RS/(H/K_{42} + q \cdot H/K_{420})$$

where $q = k_{15}/k_{51}$. The observations suggest that the translocation rates (k_{15}, k_{51}), and the proton binding to the inhibitory modifier site (K_{42}, K_{420}) are unchanged after dansylation. The transport rate at high pH values is slightly increased after dansylation. This limiting case is represented by

$$J_{max}^{S} = k_{15} \cdot RS \cdot H/(K_{32} + q \cdot K_{320})$$

This behaviour suggests that the proton binding to the stimulatory modifier site of the anion carrier saturated with SO_4^{2-} is slightly increased after dansylation (viz. K_{32}, K_{320} slightly decreased).

The pH dependence of SO_4^{2-} equilibrium exchange as measured at low SO_4^{2-} concentrations and in the absence of Cl^- has changed markedly after dansylation

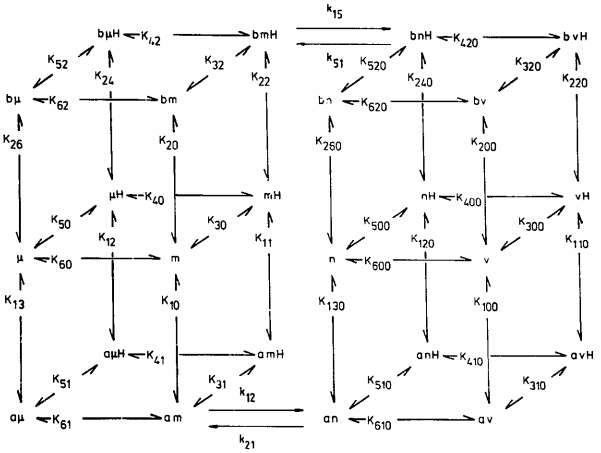

Fig. 9. Extended titratable carrier model. m, μ, and n, ν represent the conformation of the transporter with its transfer site facing the *cis* and *trans* surface of the membrane, respectively. The binding of Cl^- or SO_4^{2-} to the transfer site is designated by the addition of a · r b, respectively, to the left of m, μ, n, ν. When a proton has bound to the H^+ binding site which inhibits both Cl^- and SO_4^{2-} transport, m and n are transformed into μ and ν, respectively. The conformers with a proton bound to the H^+ binding site which inhibits Cl^- transport and enhances SO_4^{2-} transport are designated by the addition of H to the right of m, μ, n, ν. Capital K's represent the dissociation constants according to the mass law. k_{12}, k_{15}, and k_{21}, k_{51} represent the rate constants for Cl^- and SO_4^{2-} transport from the *cis* to *trans* of the membrane and vice versa, respectively.

(Fig. 4). The transport rate in the dansylated cells increases with increasing pH until a plateau or maximal value at about pH 8 is reached. For technical reasons, however, it is not possible to measure equilibrium exchange at pH values higher than 8–8.5. The transport rate in unmodified cells exhibits a maximal value at pH 6.5. In terms of the kinetic scheme (Fig. 9), the transport rate at low SO_4^{2-} and low H^+ concentrations is described by

$$J^{S}_{max} \cdot b/K_M = k_{15} \cdot RS \cdot H \cdot b/(K_{22} \cdot K_{30} + q \cdot K_{220} \cdot K_{300})$$

The altered pH dependence after dansylation suggests that the binding of SO_4^{2-} to the protonated carrier (represented by K_{22}, K_{220}), or the binding of H^+ to the carrier without any anion bound to the transfer site (represented by K_{30}, K_{300}), or both, are markedly increased after dansylation. From the relationship $K_{22} \cdot K_{30} = K_{20} \cdot K_{32}$ and $K_{220} \cdot K_{300} = K_{200} \cdot K_{320}$ it may be inferred that the binding of SO_4^{2-} to the deprotonated carrier (represented by K_{20}, K_{200}) should be considerably increased by dansylation.

The pH dependence of Cl^- equilibrium exchange as measured at high Cl^- concentrations and in the absence of SO_4^{2-} represents the pH dependence of J^{Cl}_{max} of Cl^- transport

$$J^{Cl}_{max} = V'' \cdot K''_H/(K''_H + H + H^2 \cdot K''_{HH})$$

$$V'' = k_{12} \cdot RS/(1 + p)$$

where

$$p = k_{12}/k_{21}$$

$$K''_H = (1 + p)/(1/K_{31} + 1/K_{61} + p/K_{310} + p/K_{610})$$

and

$$K''_{HH} = (1/K_{31} \cdot K_{61} + p/K_{310} \cdot K_{610})$$
$$/(1/K_{31} + 1/K_{61} + p/K_{310} + p/K_{610})$$

The effects of dansylation on the pH dependence of J^{Cl}_{max} suggest that the translocation rate of Cl^- (repre-

sented by k_{12}, k_{21}) is decreased and that K''_H is only slightly affected by dansylation.

The SO_4^{2-}/H^+ cotransport (J^{HS}) as measured at high SO_4^{2-} concentrations in exchange with high concentrations of Cl^- is approximated by

$$J^{HS} = k_{15} \cdot RS \cdot H \cdot K_{42} / (H^2 + H \cdot (K_{42} + K_{52}) + K_{42} \cdot K_{32})$$

The SO_4^{2-}/H^+ cotransport measured at the high H^+ concentration used in the present experiments is approximated by

$$J^{HS} = k_{15} \cdot RS \cdot K_{42} / H$$

and remains essentially unaltered after dansylation (Figs. 7 and 8). This is in accordance to the suggestions mentioned earlier that k_{15} and K_{42} are hardly affected by dansylation. However, the model would predict that the SO_4^{2-}/H^+ cotransport is most enhanced after dansylation when measured at low H^+ and SO_4^{2-} concentrations. In that case, SO_4^{2-}/H^+ cotransport is approximated by

$$J^{HS} = k_{15} \cdot RS \cdot b \cdot H / K_{22} \cdot K_{30}$$

For technical reasons, however, we were not able to test this prediction.

Summarizing, the observations may be explained by an extended form of the titratable carrier model as shown in Fig. 9 suggesting that dansylation: (i) increases the H^+ binding to the carrier without an anion bound to the transfer site; (ii) increases the affinity of the stimulatory H^+ binding site slightly and does not affect the affinity of the inhibitory H^+ binding site, when the transfer site is saturated with SO_4^{2-}; (iii) increases the SO_4^{2-} binding to the protonated carrier and, even more, the SO_4^{2-} binding to the unprotonated carrier; (iv) increases the Cl^- binding to the unprotonated carrier (as inferred from the concentration dependence at pH 7.4, which is not shown here); (v) does not affect the translocation rate of SO_4^{2-}, (vi) decreases the translocation rate of Cl^-. In contrast to earlier reports [25], the data do not necessarily suggest that there is no relationship between the pH dependence of SO_4^{2-} equilibrium exchange and H^+/SO_4^{2-} cotransport.

Exposure of the red cell membrane to dansyl chloride leads to the modification of many amino acid residues on band 3 [5]. So far, it was possible to demonstrate the existence of three different types of modifiable sites that upon dansylation are involved in eliciting the changes observed in anion transport. However, since many amino acid residues in addition to those of functional interest, become dansylated, it was not yet possible to identify those that are of functional significance. This also applies to the amino acid residues that become susceptible to dansylation only when the exposure to dansyl chloride takes place in the presence of the reversibly binding anion transport inhibitor APMB.

In a recent publication, Jennings and Al-Rhaiyel [26] have pointed out that the inverse effects of dansylation on Cl^- and SO_4^{2-} equilibrium exchange resemble those seen after modification with Woodward's reagent K, which modifies glutamate residues in the 28 kDa C-terminal region of band 3. We are tempted to speculate that a specific lysine or imidazole residue forms a hydrogen bond with the carboxyl group of an adjacent glutamic acid residue. Breaking this bond by either dansylation or treatment with Woodward's reagent K may lead to the same results: an enhancement of SO_4^{2-} transport and a reduction of halide transport.

References

1 Ku, C.P., Jennings, M.L. and Passow, H. (1979) Biochim. Biophys. Acta 553, 132–144.
2 Lepke, S. and Passow, H. (1982) J. Physiol. (London) 328, 27–48.
3 Seiler, N. (1970) in Methods of Biochemical Analysis, Vol. 18 (Glick, D., ed.), pp. 259–336, John Wiley and Sons, New York.
4 Schmidt-Ullrich, R., Knüfermann, H. and Wallach, D.F.H. (1973) Biochim. Biophys. Acta 307, 353–365.
5 Raida, M. and Passow, H. (1985) Biochim. Biophys. Acta 812, 624–632.
6 Knauf, P.A. (1979) Curr. Top. Membr. Transp. 12, 249–363.
7 Macara, I.G. and Cantley, L.C. (1983) in Cell Membranes: Methods and Reviews, Vol. 1 (Elson, E., Frazier, W., Glaser, L., eds.), pp. 47–87, Plenum Press, New York.
8 Jennings, M.L. (1985) Annu. Rev. Physiol. 47, 519–533.
9 Passow, H. (1986) Rev. Physiol. Biochem. Pharmacol. 103, 61–203.
10 Funder, J. and Wieth, J.O. (1976) J. Physiol. (London) 262, 679–698.
11 Brahm, J. (1977) J. Gen. Physiol. 70, 283–306.
12 Schwoch, G., Rudloff, V., Wood-Guth, I. and Passow, H. (1974) Biochim. Biophys. Acta 339, 126–138.
13 Schnell, K.F., Gerhardt, S., Schöppe-Fredenburg, A. (1977) J. Membr. Biol. 30, 319–350.
14 Gunn, R.B. (1972) in Oxygen Affinity of Hemoglobin and Red Cell Acid Base Status (Rorth, M. and Astrup, P., eds.), pp. 823–827, Munksgaard, Copenhagen.
15 Gunn, R.B. (1973) in Erythrocytes, Thrombocytes, Leucocytes (Gerlach, E., Moser, K., Deutsch, E. and Wilmanns, W., eds.), pp. 77–79, Thieme, Stuttgart.
16 Gunn, R.B. (1979) in Membrane Transport in Biology, Vol. 2 (Giebisch, G., Tosteson, D.C. and Ussing, H.H., eds.), pp. 59–80, Springer Verlag, Berlin.
17 Jennings, M.L. (1976) J. Membr. Biol. 28, 187–205.
18 Legrum, B., Fasold, H. and Passow, H. (1980) Hoppe-Seyler's Z. Physiol. Chem., 361, 1573–1590.
19 Berghout, A., Raida, M., Romano, L. and Passow, H. (1985) Biochim. Biophys. Acta 815, 281–286.
20 Schwoch, G. and Passow, H. (1973) Mol. Cell. Biochem. 2, 197–218.
21 Dalmark, M. and Wieth, J.O. (1972) J. Physiol. (London) 244, 583–610.
22 Kachel, V. (1979) in Flow Cytometry and Sorting (Melamed, Mullaney and Mendelsohn, eds.), pp. 61–104, John Wiley and Sons, New York.
23 Milanick, M. and Gunn, R.B. (1982) J. Gen. Physiol. 79, 87–113.
24 Milanick, M. and Gunn, R.B. (1984) Am. J. Physiol. 247, C247–C259.
25 Berghout, A., Raida, M., Legrum, B. and Passow, H. (1988) Naunyn-Schmiedeberg's Arch. Pharmacol. 338, R29.
26 Jennings, M.L. and Al-Rhaiyel, S. (1988) J. Gen. Physiol. 92, 161–178.